

PACS numbers: 52.38.Mf; 52.50.Jm; 42.65.Re; 42.62.Cf
DOI: 10.1070/QE2014v044n03ABEH015054

Thermophysical and gas-dynamic characteristics of laser-induced gas-plasma flows under femtosecond laser ablation of titanium in vacuum

E.Yu. Loktionov, Yu.S. Protasov, Yu.Yu. Protasov

Abstract. **We report the results of experimental investigation of thermophysical and gas-dynamic characteristics of the gas-plasma flows induced by ultrashort (45–60 fs) laser pulse irradiation (the radiation wavelength λ = 400, 800 nm) of a titanium target in vacuum (~5×10^{-4} mbar). The use of combined interferometric technique and complex experimental data processing allowed us to estimate the momentum coupling coefficient ($C_m \sim 10^{-4}$ N W^{-1}), the efficiency of laser energy conversion to the kinetic energy of the gas-plasma flow (65%–85%), the spatiotemporal distributions of the particle density ($n_e = 10^{18}$–10^{20} cm^{-3}) and velocity ($\langle v \rangle$ = 4–9 km s^{-1}), the static (10^6–10^8 Pa) and total (10^7–10^{11} Pa) pressure and temperature (T = 7–50 kK) in the flow. Our data are compared with published data obtained by other methods.**

Keywords: *laser ablation, combined interferometry, gas-plasma flows, electron density, temperature, pressure, conversion efficiency, vacuum, titanium.*

1. Introduction

The interest in investigating the femtosecond laser ablation of technologically significant materials is steadily growing due to several advantages offered by ultrashort pulse irradiation, which arise primarily from the fact that the duration of optical irradiation is shorter than the electron-phonon relaxation time [1]. This leads to a significant lowering of the fraction of dissipated heat and therefore to a shortening of the zone of thermal action [2], i.e., to an increase in volume energy density in the target substance. This is especially important for refractory metals and metals with a high thermal conductivity, because it substantially improves the efficiency of micromachining [3] and gas-plasma flow production [4] as well as the resolving power of analytical methods [5], etc. In this connection the study of thermophysical and gas-dynamic processes in the femtosecond laser ablation is topical both from the general-physical and applied standpoints.

The experimental investigation of gas-plasma flows driven by ultrashort laser pulse irradiation of condensed media has several special features arising mainly from the low energies of irradiation pulses and therefore from the small characteristic linear dimensions of the gas-plasma flow and its emission intensity [6]. When use is made of diagnostic equipment and techniques with insufficient sensitivity or spatiotemporal resolution, the quantitative processing of measurement data is limited or impossible [7]. For instance, photorecording methods [8, 9] can most often yield only qualitative data or spatially 0–1-dimensional (and most often time-integrated, i.e. with exposure times much longer than the duration of characteristic processes) emission spectra [10]. Interferometric techniques, which provide the required spatiotemporal resolution, are infrequently employed owing to their complexity. Processing the experimental data obtained with their aid is also rather difficult and therefore is sometimes incomplete [8, 11].

More often the mathematical models of femtosecond laser ablation of metals are employed to consider the processes at the surface or in the bulk of the target [12–18] and more rarely in the near-surface region [19], but in all cases the time intervals under investigation amount to several picoseconds. The more elaborate gas-plasma models constructed to describe the action of nanosecond pulses (see, for instance, Refs [20–23]) are of limited usefulness in this case, because the metal vaporisation takes place not in the course of laser irradiation, but immediately after it and prior to the development of a macroscopic gas-plasma flow.

The high specific cost of the pulse and the arduousness of the maintenance of high-power femtosecond laser facilities limit the investigation of substances with high spectral-energy thresholds of laser ablation. Among refractory metals, one of the lowest thresholds of laser ablation under ultrashort-pulse irradiation is inherent in titanium [24], and the scope of its technological applications is quite broad. Our resultant data are of significance in developing laser-plasma thrusters [25], gas-plasma flow injectors [26], laser-induced forward transfer technologies [27], microelectromechanical systems [28] and thin-film coating deposition methods [29].

The objective of our work is to investigate the thermophysical and gas-dynamic processes in the gas-plasma flows produced by ultrashort-pulse laser irradiation of titanium targets in vacuum; in this case, use is made of combined pulsed laser interferometry [30] together with the bundled software for automated experimental data processing [31].

2. Experimental facility and method of investigation

Our experimental facility involving a terawatt femtosecond laser complex (radiation wavelength λ = 266, 400 and 800 nm; half-height pulse duration $\tau_{0.5}$ = 70, 60 and 45 fs; irradiation intensity I_0 up to 2.1×10^{13}, 2.5×10^{14} and 9.4×10^{15} W cm^{-2}, respectively) as well as the methods of research and its data processing are described at length in Refs [30–32]; the results

E.Yu. Loktionov, Yu.S. Protasov, Yu.Yu. Protasov N.E. Bauman Moscow State Technical University, 2nd Baumanskaya ul., 5, 105005 Moscow, Russia; e-mail: stcpe@bmstu.ru

Received 9 November 2012; revision received 13 January 2014
Kvantovaya Elektronika **44** (3) 225–232 (2014)
Translated by E.N. Ragozin

of a similar experiment on the irradiation of polymer materials are presented in Ref. [33]. The use of the method for the complex processing of surface (Michelson scheme) and near-surface (Mach–Zehnder scheme) target region interferometry proposed in Refs [31, 32] permitted determining the material mass flow from the target surface and the electron density distribution in the laser-induced gas-plasma flow. Proceeding from these data, an estimate was made of the particle velocity distribution for the ionised component ($n_e = 10^{18}-10^{20}$ cm^{-3}), which makes the main contribution to the formation of recoil momentum*.

Using these primary data as the base, we estimated the spatiotemporal distributions of the thermophysical and gas-dynamic parameters (the electron density, the static and total pressure, the temperature) of the near-surface gas-plasma flow and several integral parameters characterising the efficiency of laser energy conversion to the kinetic energy and mechanical momentum, and also estimated the average degree of ionisation ($\alpha \sim 0.4-1.9$).

For targets we used thin films (with thicknesses of 200–400 nm and a reflectivity $R_{800} \sim 0.39$) deposited by magnetron sputtering on glass substrates, and massive samples of BT1-0 (State Standard 19807–91, with Ti content of 99.24%–99.7%) titanium alloy polished mechanically to a surface roughness of ~0.2 μm.

In the processing of combined interferometry data, use was made of several basic relations. The electron density [35]

$$n_e \approx \frac{8\pi^2 c^2 \varepsilon_0 m_e n_0}{\lambda^2 e^2}\Delta n \approx 2.23\times 10^{15}\frac{\Delta n}{\lambda^2},$$

where c is the speed of light in vacuum; ε_0 is the dielectric constant; m_e is the electron mass; n_0 is the refractive index of the buffer gas; λ is the probe radiation wavelength; e is the electron charge; and Δn is the change of the refractive index in the medium.

As is well known [36], the change in the refractive index of a gas-plasma flow is determined by the densities of positively and negatively charged particles as well as of neutral ones; when the flow is dominated by one sort of particles, the contribution of the other is neglected. In accordance with Ref. [37], we assumed that the electron contribution prevails, because $n_e/n_a > 0.3$, where n_a is the atomic density; however, the local degree of ionisation may significantly vary with distance from the target surface, which may affect the correctness of analysis.

One of the characteristic parameters in the production of gas-plasma flows is their lifetime. The axial dimension of the laser ablation plume exceeded the radiation focal spot size $d_0 = 40 \pm 2.4$ μm (at a $1/e^2$ level and an incidence angle of 45°) in $\Delta t \sim 10^{-8}$ s after target irradiation. The gas-plasma flow lifetime is determined by the processes occurring in it or by the threshold level of some of its characteristics. In our case, the characteristic in point was the electron density ($n_e \sim 10^{17}$ cm^{-3}), which gave rise to a change in refractive index detectable by interferometric techniques; the thus determined gas-plasma flow lifetime Δt was equal to ~10^{-7} s.

* For similar regimes of titanium target irradiation in vacuum in Ref. [34], nanoclusters were not recorded in the nanosecond delay range and the gas-plasma flow was well collimated; however, in the 5–50 μs delay range it possessed a wide divergence and consisted primarily of clusters. Therefore, the effect of nanoparticles may be neglected for the 12–75 ns delay range under our investigation.

The temperature was estimated by the integral formula for the linear absorption coefficient k [38]:

$$k = \frac{4}{3}\left(\frac{2\pi}{3m_e k_B T}\right)^{1/2}\frac{z_i^2 e^6}{\hbar c m_e \omega_0^3} n_i n_e \exp\left(\frac{\hbar\omega_0}{k_B T}\right), \quad (1)$$

where ω_0 is the absorbed photon frequency; z_i is the ion charge; and T is the electron temperature (under local thermodynamic equilibrium $T \sim T_e \sim T_i$).

The mass averaged longitudinal particle velocity

$$\langle V_{long}\rangle = \frac{\sum_k n_e^k V_{long}^k}{\sum_k n_e^k},$$

where $V_{long}^i = L/t$ is the particle velocity averaged over a time t; L is the particle–target distance at the point in time t; and n_e^k is the electron density in an elementary volume. The similarity of electron and ion velocity distributions in a gas-plasma flow produced by femtosecond laser irradiation was experimentally demonstrated in Ref. [39], and the local electron density was therefore taken as a weight function in the estimation of particle velocity distribution. The static and total pressures were defined as $p_e = n_e k T_e$ and $p_e^* = p_e + m_e n_e V_e^2/2$, respectively.

The momentum coupling coefficient [25]

$$C_m = \frac{1}{E}\int F(t)\,dt \approx \frac{\Delta m\langle v\rangle}{E},$$

where E is the energy of a laser pulse; F is the tractive force; and $\langle v\rangle$ is the velocity. It is noteworthy that the majority of measurement techniques (using acceleration [40], force [41], and pressure [42, 43] sensors, pulsed pendulums [44]) traditionally employed in this case cannot be employed to directly measure the tractive characteristics under femtosecond laser ablation due to their insufficient sensitivity: produced under single microjoule irradiation are superlow (below 10^{-8} N s) recoil momenta, whose recording is restrictedly possible only using torsion pendulums [45] (for a more comprehensive analysis of the capabilities of these methods, see Refs [32, 46]). In view of this, the employment of an indirect, but more informative method – the combined interferometry of the target surface and the near-surface region – is justified.

The efficiency of laser ablation may be determined by taking into account different forms of energy in which the laser radiation is converted and the energy stored in the target substance. Used most often is the ratio between the kinetic energy of directional particle motion in the gas-plasma flow and the energy of the laser pulse – the tractive efficiency of laser ablation [25]:

$$\eta = \frac{\sum mv^2}{2E} \approx \frac{\Delta m\langle v\rangle^2}{2E} \approx \frac{gC_m I_{sp}}{2},$$

where $I_{sp} = \sum mv/\sum mg \approx \langle v\rangle/g$ is the specific impulse and $g = 9.81$ m s^{-2} is the free fall acceleration.

The efficiency of kinetic energy conversion to the useful work of recoil momentum production is determined by particle velocity dispersion and is characterised by the degree of monochromaticity (collimation) of the gas-plasma flow, or the tractive-to-energy efficiency ratio [47]:

$$\mu = \frac{\sum m v_z^2}{\sum m v^2} \approx \frac{\langle v \rangle^2}{\langle v^2 \rangle},$$

where v_z is the particle velocity projection on the gas-plasma flow axis (in the case of axial symmetry, $\langle v_z \rangle = \langle v \rangle$).

The spatial resolution of interferometers was equal to ± 0.8 μm, the limiting time resolution of the optical setup was about 10^{-13} s and the resolution in determining the mass flow was $\sim 10^{-11}$ g [30]. The automated data processing impairs the spatial resolution by an order of magnitude in comparison with the data recorded experimentally. The uncertainty in determining mass averaged velocity Δv was equal to ~ 350 m s^{-1}.

3. Experimental results and their discussion

The specific mass flow under laser ablation is the key characteristic in determining its efficiency. Under second harmonic irradiation the m/E values are significantly higher than under irradiation by the fundamental frequency [24]; in the latter case, observed for $W \approx 6$ J cm^{-2} was a transition from a low-energy irradiation regime to a high-energy regime (Fig. 1) [48] (under normal atmospheric conditions, a shock wave in the air becomes detectable at this radiation energy density). A similar transition was observed in the picosecond laser ablation of refractory metals in Ref. [49] and of a titanium alloy in Ref. [50]. Under ultrashort laser pulse irradiation in vacuum, the absolute values of the specific mass flow (10^{-5}–10^{-4} g J^{-1}) are significantly high than under nanosecond pulse irradiation ($\sim 10^{-6}$ g J^{-1} [51]), although the laser ablation thresholds are little different in these regimes [24]. Unlike nanosecond pulse irradiation, the specific mass flow for metals approaches that for polymers [52].

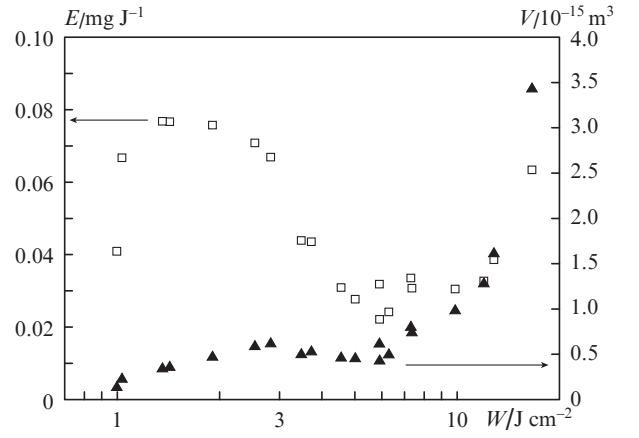

Figure 1. Dependences of the specific mass flow (squares) and ablation crater volume (triangles) on the laser energy density ($\lambda = 800$ nm).

As shown below, a higher mass flow under femtosecond irradiation gives rise to higher values of electron density, mechanical recoil momentum and efficiency of laser energy conversion to the kinetic energy of the gas-plasma flow. Furthermore, the high efficiency of laser energy conversion is attested by the fact that the specific mass flow approaches the reciprocal of the sublimation energy, which is calculated as the sum of the latent heat of melting, heat of vaporisation, and the heat required to heat the substance from the melting temperature to the boiling temperature. The specific mass flow in our work is somewhat higher that the published data for similar irradiation regimes; the most probable explanation for this fact is the use of thin film targets in our work, which further limits the heat dissipation under femtosecond irradiation. This assumption is partly borne out by the data of Ref. [53], where the ablation crater depth was shown to be inversely proportional to the film target thickness in the case of steel.

The velocity characteristics of laser-induced gas-plasma flows have been studied in many works, but the data most often pertain only to charged particles [45, 54], a fraction (undetermined, as a rule) of which possesses high velocities (aver 10^4–10^5 m s^{-1} [55]). More often the particle velocity distribution is satisfactorily described by the summation of two or three Maxwellian functions corresponding to neutral particles and ions of different charge state. Proceeding from the Maxwellian particle velocity distribution, for particles with energies corresponding to ionisation energies E_i (these are 6.83, 13.57, and 27.52 eV [56] for the three first Ti ions, $M_{Ti} = 47.88$ g mole^{-1}) the most probable velocity $v_p = (2N_a E_i/M)^{1/2}$ (Fig. 2) and the mass averaged velocity $\langle v \rangle = (8N_a E_i/\pi M)^{1/2}$ (Fig. 3).

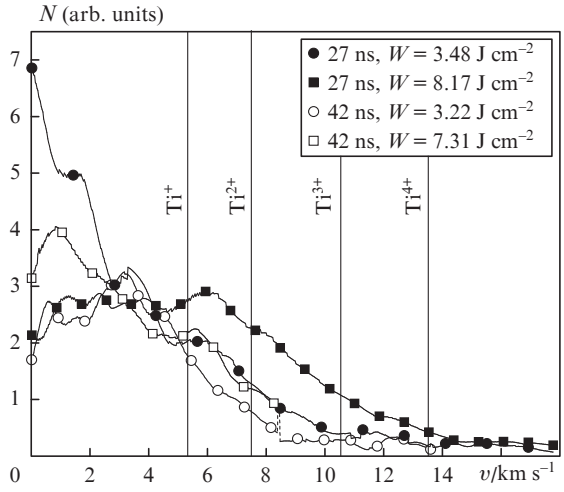

Figure 2. Particle velocity distribution in a gas-plasma flow and calculated values of the most probable ion velocities (indicated by vertical lines).

In the emission spectra (Fig. 4) of the gas-plasma flow there are lines of doubly ionised titanium ions and the mass averaged particle velocities (Fig. 3) for $W \sim 20$ J cm^{-2} are lower than those of Ti^+ ($\langle v \rangle_{Ti^+} = 10.48$ km s^{-1}). No ions of charge 2^+ were observed under irradiation by nanosecond pulses with a similar energy density in Ref. [6] (it is hypothesised that the reason may also lie with the masking of their weak lines by the continuum).

Titanium is one of the lightest metals, and relatively high particle expansion velocities would therefore be expected to occur in the gas-plasma flow. Figure 2 shows the particle velocity distributions, in which two peaks stand out; they correspond to the most probable velocities of atoms and singly charged ions [57] in accordance with the Maxwellian particle velocity distribution at temperatures of 1–3 eV. Similar results were obtained under similar experimental conditions by photometry of the gas-plasma flow images in Ref. [7]; in

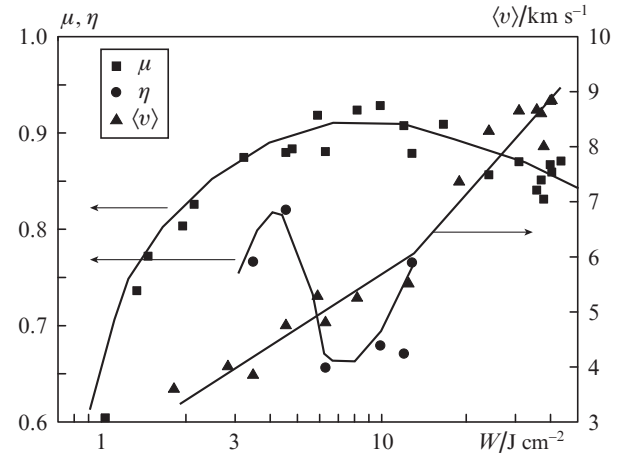

Figure 3. Dependences of the degree of monochromaticity (μ), thrust efficiency (η) and mass averaged particle velocity ($\langle v \rangle$) of the gas-plasma flow on the laser energy density (λ = 800 nm).

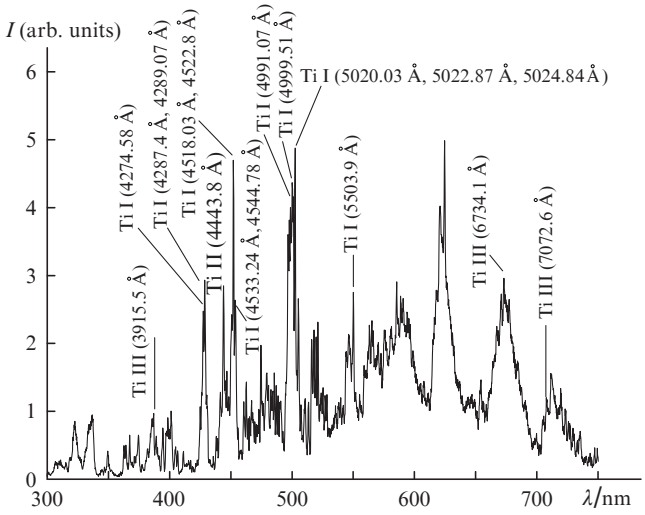

Figure 4. Integral emission spectrum recorded in the femtosecond laser ablation of a Ti target under atmospheric conditions (λ = 800 nm, $W \sim$ 40 J cm^{-2}).

that work the mass averaged particle velocities measured with a time-of-flight probe are in agreement with our measurement data. Evidently the fraction of high-velocity particles increases with irradiation energy, resulting in an increase in mass averaged particle velocity (see Fig. 3). In this case, the particle velocity somewhat lowers with time for the same irradiation intensity (see Fig. 2). This result is most likely due to the fact that the particle density in the distal (high-velocity) part of the flow falls below the sensitivity threshold with time and thereby drops out of the calculation.

Proceeding from the qualitative analysis of holographic interferograms of laser-ablation plumes, in Ref. [9] a conclusion was drawn about the presence of particles with a high momentum and a velocity direction close to the target surface normal (which corresponds to a high degree μ of flow monochromaticity [47]). The data in Fig. 3 qualitatively confirm this assumption. In this case, the dependence shows an optimum near the low-to-high energy ablation transition point [58, 59]. The efficiency of conversion of gas-plasma flow kinetic energy to the mechanical recoil momentum is characterised by the degree of monochromaticity, which, as a rule, is not presented as an integral coefficient in publications concerned with the particle angular velocity distribution [60–62]. In the mentioned papers, to estimate these characteristics use is made of the exponent n in the approximative dependence $v(\theta) = v_0 \cos^n \theta$ (although it would be more correct to assume $v(\theta) = a + b\cos^n \theta$ [63] or a more complex function). A qualitative analysis of the results of these works suggests that an ultrashort pulse irradiation produces a better collimated laser ablation flux than under nanosecond pulse irradiation. As shown in Ref. [61], the degree of monochromaticity in the case of nanosecond pulse irradiation is proportional to the thermophysical metal characteristics like the sublimation energy as well as the melting and boiling temperatures. However, our data do not exhibit such dependences, probably due to the change of ablation mechanism [64] and a narrower range of these temperatures in our case.

Figure 5a shows the characteristic electron density distribution in the gas-plasma flow and Fig. 5b illustrates the dependence of this parameter distribution along the flow axis on the laser energy density and the time delay of exposure relative to the instant of irradiation. These results are in good

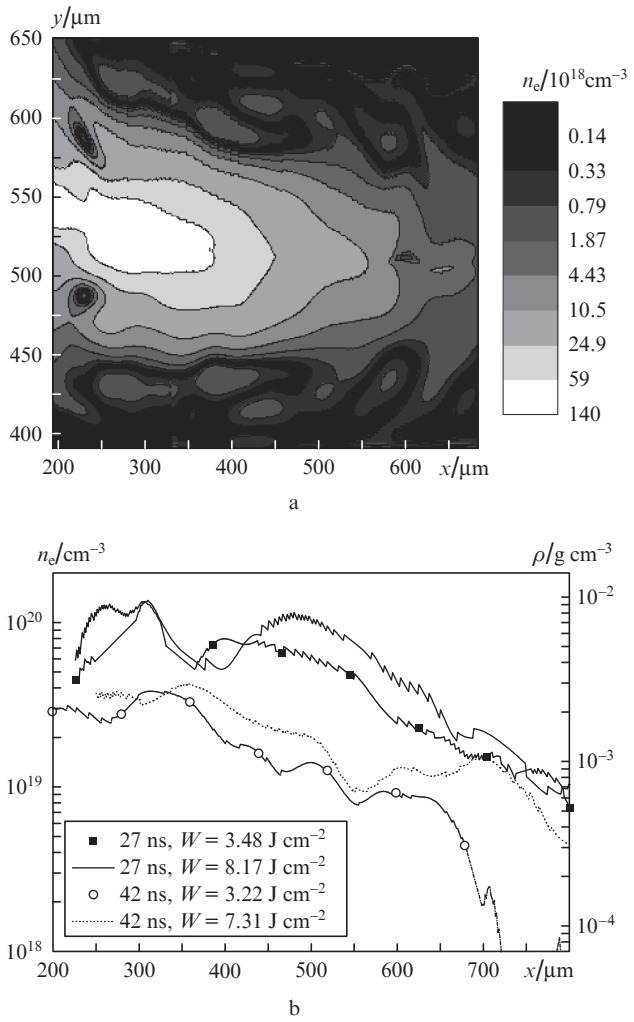

Figure 5. Spatial distributions of the electron density n_e and the density ρ at the middle section of the gas-plasma flow (a) and along its axis (b) (from here on, unless otherwise stated, for the in-vacuum Ti target $p \sim 10^{-3}$ Pa, λ = 800 nm, W = 5.09 J cm^{-2}, λ_{prob} = 400 nm in 27 ns after laser irradiation).

agreement with the data obtained by emission spectroscopy methods under similar conditions [10] (the fundamental equivalence of the data obtained by both methods under the same condition was experimentally borne out in Ref. [65]) and are somewhat higher than the values obtained under irradiation by nanosecond pulses [66] owing to a higher specific mass flow and a higher temperature. Although the local values of the electron density depend only slightly on the radiation energy density in the range investigated, they decrease with time due to gas-plasma flow expansion, especially in its distal part (the volume integrals of the electron density taken 27 and 42 ns after laser irradiation are hardly different, i.e. recombination may be neglected during this time interval). Under the assumptions made, the density distribution is qualitatively similar to the electron density distribution with a scale factor of $\sim 7\times10^{-23}$ g, which gives higher values than the air density at normal conditions, and the density gradient amounts to ~1 g cm^{-4}. The product of the local values of electron density and particle velocity gives an estimate of potential current density of 10^6-10^7 A cm^{-2} – higher than in an arc discharge; in the deceleration of this flow in the electric field it is possible to obtain a high-brightness light source with an emission peak in the short-wavelength part of the spectrum [67, 68].

The characteristic spatial distribution of the temperature in the gas-plasma flow is shown in Fig. 6a, and Fig. 6b shows the dependence of its distribution along the flow axis on the laser energy density and the time delay of exposure relative to the instant of irradiation. One can see that the temperature in the flow axis 27 ns after irradiation and in the proximal (closest to the target) part of the flow 42 ns after irradiation depends only slightly on the energy of radiation pulses. The emergence of appreciable differences in electron density and temperature in the distal part of the flow 42 ns after irradiation for different irradiation intensities is attributable to a difference in particle expansion velocities (for a shorter exposure delay this difference is less pronounced). The range of temperature values corresponds to the data of Refs [10, 69] obtained by emission spectroscopy techniques under similar experimental conditions. The temperatures recorded in the in-vacuum irradiation are significantly higher than in atmospheric conditions [70].

The acquisition of the spatiotemporal distributions of static and total pressures in a gas-plasma flow is a unique result for the experimental investigations of laser–matter interactions. As a rule, measurements in such experiments are made of the pressure produced within the target thickness ($p = 10^{11}-10^{12}$ Pa) [71, 72]. The data presented in Fig. 7 correspond to theoretical estimates for the case of femtosecond pulse irradiation [73]. The static pressure ranges up to 10^8 Pa, which is comparable to the pressure at the front of a shock wave produced in the nanosecond irradiation in normal atmospheric conditions [74] and in water [75] and exceeds this parameter in the femtosecond irradiation of polymers [33].

Experimental data on the momentum coupling coefficient produced by the femtosecond laser pulse irradiation of titanium targets are missing in the literature. Among refractory metals, Mo and W (Fig. 8) are available for comparison, and Ti turns out to be appreciably more efficient for tractive force generation under the same conditions. Owing to a high specific mass flow, for a clearly pronounced dependence of the mass averaged velocity on the radiation energy density the dependence of C_m shows an inflection point when the low-energy regime passes into the high-energy one. The character

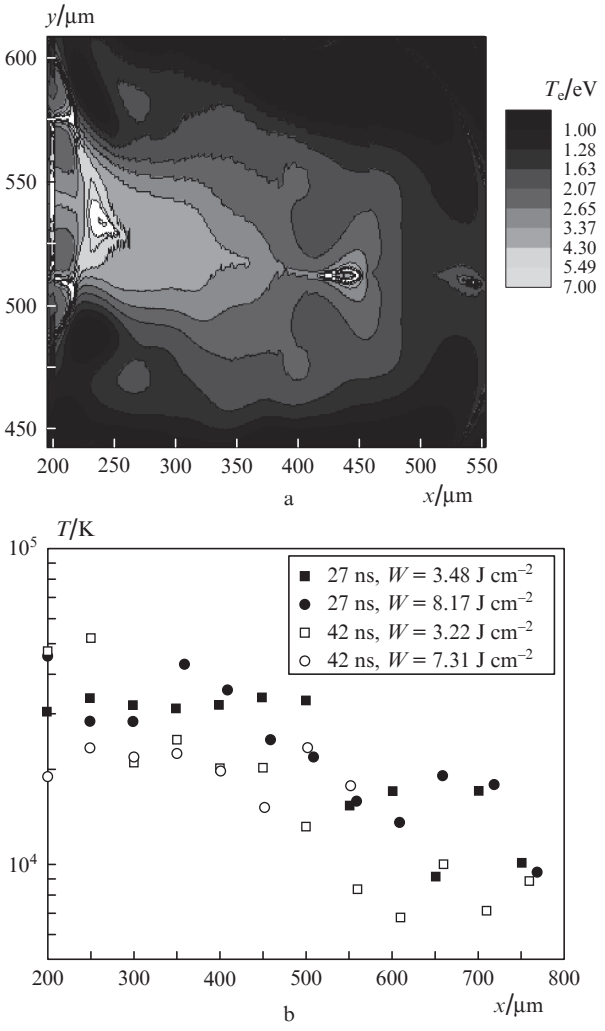

Figure 6. Spatial distributions of the temperature at the middle section of the gas-plasma flow (a) and along its axis (b) in relation to the spectral-energy irradiation parameters.

of this dependence implies the existence of two maxima – in each of these regimes. As far as we know, similar inflection points in the dependence of C_m on the intensity of laser irradiation have been recorded for the first time, whatever the material and laser irradiation parameters.

Data on the momentum coupling coefficient for Ti and its alloys are available in a broad irradiation parameter range (Fig. 8). Unlike polymers [76, 77] and aluminium alloys, under micro- or nanosecond pulse irradiation [78] C_m is directly proportional to the complex irradiation parameter $I_0\lambda\tau^{0.5}$ in a broad range of laser pulse durations. This dependence may be explained as follows: for a higher-intensity irradiation, less heat dissipates and more heat is transferred to the ablated particles. Furthermore, the laser ablation thresholds W_a decrease proportionally to $\tau^{-1/2}$ until the radiation pulse duration τ reaches the electron-phonon relaxation time [24, 45], i.e. the maxima of parameters that are proportional to the ratio W/W_a shift to the side of lower-energy irradiation.

Data on the efficiency of laser energy conversion to the kinetic energy of a gas-plasma flow generated by ultrashort-pulse irradiation of metallic targets are scarce in the literature. For a nanosecond IR pulse irradiation in Ref. [4] it was determined that η varies in the $7.5\times10^{-3}-1$ range for gold in vacuum; for titanium in atmospheric conditions η ranges

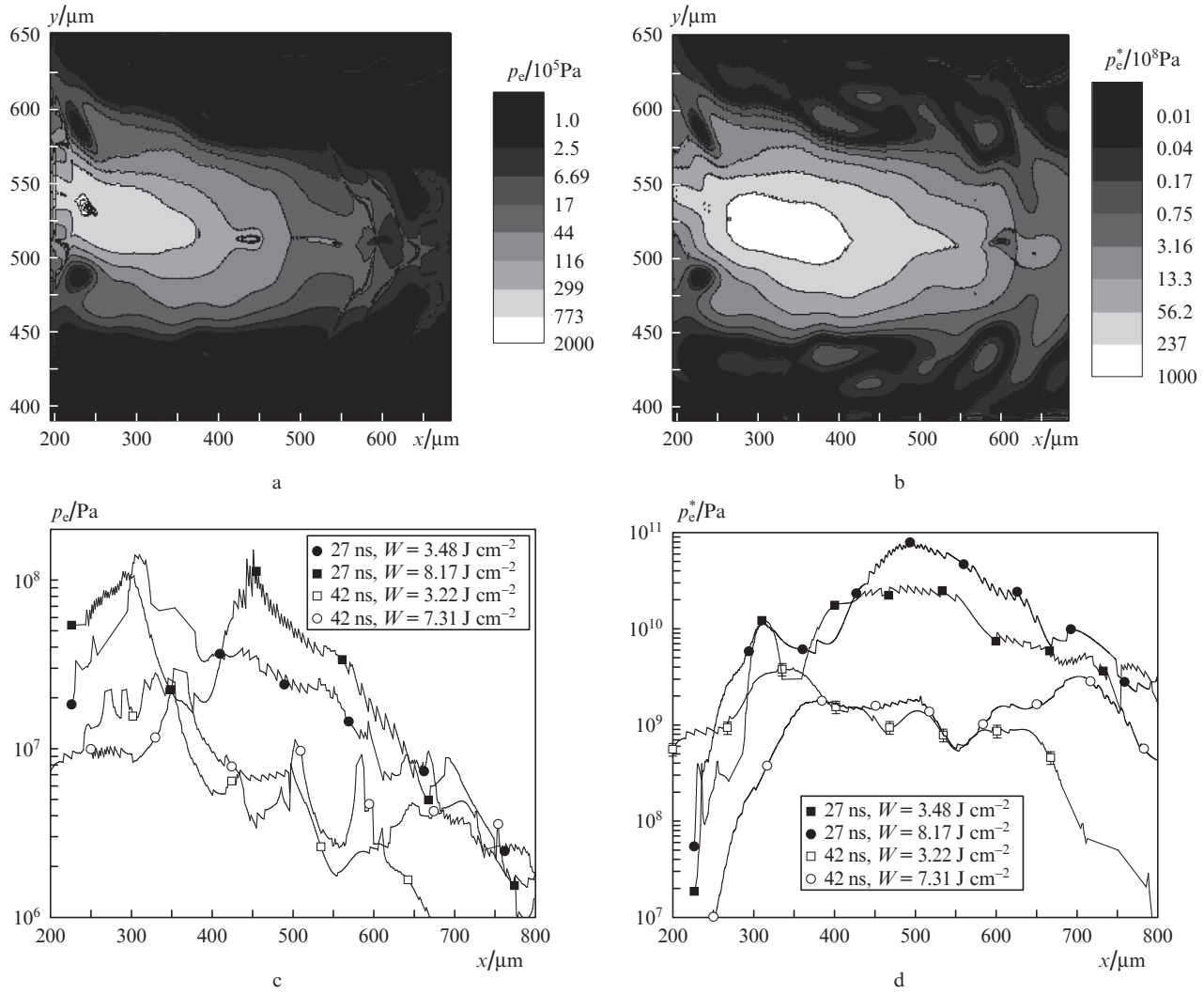

Figure 7. Spatial distributions of the static (a, c) and total (b, d) pressures at the middle section of the gas-plasma flow (a, b) and along its axis (c, d) in relation to the spectral-energy irradiation parameters.

from 0.055 to 0.15 [79]. Similarly to C_m, the η(W) dependence has an inflection point and two maxima are expected to exist; in this case, in absolute figures the maxima of C_m and η are closer to each other in the low-energy irradiation regime than in the high-energy one. The existence of inflection significantly broadens the range of laser irradiation regimes acceptable from the standpoint of efficiency.

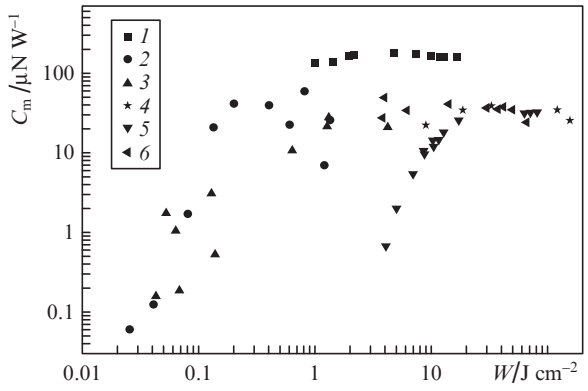

Figure 8. Dependences of the momentum coupling coefficient on the spectral-energy irradiation parameters: our data for Ti (*1*), as well as for Mo [80] (*2*), W [45] (*3*), TA6V (248 nm, 400 ns, vacuum) [81] (*4*), Ti5A14V (350 nm, 500 ns, vacuum) [82] (*5*), and Ti6A14V (3.6 μm, 7 μs) [83] (*6*).

4. Conclusions

We have experimentally determined several thermophysical and gas-dynamic characteristics of the gas-plasma flows produced by irradiating a plane target in vacuum with ultrashort laser pulses. Unlike the majority of similar works, we have obtained the spatiotemporal distributions of the electron density (10^{18}–10^{20} cm^{-3}), temperature (7–50 kK), static (10^6–10^8 Pa) and total (10^7–10^{11} Pa) pressures. For the first time it has been possible to determine the following optomechanical characteristics in the case of ultrashort pulse irradiation of titanium: the momentum coupling coefficient ($C_m \sim 2.5\times10^{-4}$ N W^{-1}) and the efficiency of laser energy conversion to the kinetic energy of a gas-plasma flow (η = 0.65–0.85). Quantitative data on the degree of gas-plasma flow monochromaticity (μ = 0.75–0.92) testify to a high efficiency of radiation energy conversion to the energy of directional par-

ticle motion. Estimates of static and total pressure distributions in the gas-plasma flow produced by ultrashort laser pulses have been experimentally obtained for the first time.

Acknowledgements. The authors express their appreciation to A.V. Ovchinnikov and D.S. Sitnikov for their aid in the pursuance of experiments on the femtosecond laser complex of the Joint Institute for High Temperatures of the Russian Academy of Sciences, to R.R. Khaziev for his aid in the automation of experimental data processing, and to V.D. Telekh for helpful remarks in the discussion of results. This work was supported by the Russian Foundation for Basic Research (Grant Nos 11-08-00843 and 12-08-12047).

References

1. Axente E., Mihailescu I.N., Hermann J., Itina T.E. *Appl. Phys. Lett.*, **99**, 081502 (2011).
2. Petite G., in *Lasers et Technologies Femtosecondes*. Ed. by Marc Sentis and Olivier P. Uteza (Saint-Etienne: PU Saint-Etienne, 2005) p. 466.
3. Gladush G.G., Smurov I. *Physics of Laser Materials Processing* (Berlin–Heidelberg: Springer, 2011).
4. Phipps C., Luke J., in *Laser Ablation and its Applications* (New York: Springer, 2007) p. 407.
5. Fantoni R., Caneve L., Colao F., Fornarini L., Lazic V., Spizzichino V., in *Advances in Spectroscopy for Lasers and Sensing* (Dordrecht: Springer Netherland, 2006) p. 229.
6. De Giacomo A., Dell'Aglio M., Santagata A., Teghil R. *Spectrochim. Acta Pt. B: Atomic Spectrosc.*, **60**, 935 (2005).
7. Grojo D., Hermann J., Perrone A. *J. Appl. Phys.*, **97**, 063306 (2005).
8. Waugh J., Gregory C., Wilson L., Loupias B., Brambrink E., Koenig M., Sakawa Y., Kuramitsu Y., Takabe H., Kodama R., Woolsey N. *Astrophys. Space Sci.*, **322**, 31 (2009).
9. Amer E., Gren P., Kaplan A.F.H., Sjodahl M., El Shaer M. *Appl. Surf. Sci.*, **256**, 4633 (2010).
10. Axente E., Noel S., Hermann J., Sentis M., Mihailescu I.N. *Appl. Surf. Sci.*, **255**, 9734 (2009).
11. Vogel N., Kochan N. *Appl. Surf. Sci.*, **127–129**, 928 (1998).
12. Khishchenko K.V., Veysman M.E., Andreev N.E., Fortov V.E., Levashov P.R., Povarnitsyn M.E. *Proc. SPIE Int. Soc. Opt. Eng.*, **7005**, 70051S (2008).
13. Yang J., Zhao Y., Zhu X. *Appl. Phys. A: Mater. Sci. Proc.*, **89**, 571 (2007).
14. Schmidt V., Husinsky W., Betz G. *Appl. Surf. Sci.*, **197–198**, 145 (2002).
15. Vestentoft K., Balling P. *Appl. Phys. A: Mater. Sci. Proc.*, **84**, 207 (2006).
16. Christensen B.H., Vestentoft K., Balling P. *Appl. Surf. Sci.*, **253**, 6347 (2007).
17. Afanasiev Y., Chichkov B., Isakov V., Kanavin A., Uryupin S. *J. Rus. Laser Research*, **20**, 189 (1999).
18. Chen J.K., Beraun J.E. *J. Opt. A: Pure Appl. Opt.*, **5**, 168 (2003).
19. Sherrill M.E., Abdallah J.J., Csanak G., Dodd E.S., Fukuda Y., Akahane Y., Aoyama M., Inoue N., Ueda H., Yamakawa K., Faenov A.Y., Magunov A.I., Pikuz T.A., Skobelev I.Y. *Proc. SPIE Int. Soc. Opt. Eng.*, **7005**, 70051R (2008).
20. Gusarov A.V., Gnedovets A.G., Smurov I. *Appl. Surf. Sci.*, **154–155**, 66 (2000).
21. Gusarov A.V., Smurov I. *J. Phys. D: Appl. Phys.*, **34**, 1147 (2001).
22. Gusarov A.V., Smurov I. *J. Phys. D: Appl. Phys.*, **36**, 2962 (2003).
23. Wu B., Shin Y.C. *Phys. Lett. A*, **371**, 128 (2007).
24. Loktionov E.Yu., Ovchinnikov A.V., Protasov Yu.Yu., Sitnikov D.S. *Zh. Prikl. Spektrosk.*, **77**, 604 (2010) [*J. Appl. Spectrosc.*, **77**, 561 (2010)].
25. Phipps C., Birkan M., Bohn W., Eckel H.-A., Horisawa H., Lippert T., Michaelis M.M., Rezunkov Y., Sasoh A., Schall W., Scharring S., Sinko J. *J. Populs. Power*, **26**, 609 (2010).
26. Malka V., Faure J., Rechatin C., Ben-Ismail A., Lim J.K., Davoine X., Lefebvre E. *Phys. Plasmas*, **16**, 056703 (2009).
27. Piqué A., Kim H., Arnold C., in *Laser Ablation and its Applications* (New York: Springer, 2007) p. 339.
28. Elbandrawy M.A.K.A. *Ph.D. thesis* (Norfolk: Old Dominion University, 2006).
29. Schneider C.W., Lippert T., in *Laser Processing of Materials*. Ed. by Peter Schaaf (Berlin–Heidelberg: Springer 2010) Vol. 139, p. 89.
30. Loktionov E.Yu., Ovchinnikov A.V., Protasov Yu.Yu., Sitnikov D.S. *Prib. Tekh. Eksp.*, (3), 104 (2010) [*Instrum. Experim. Techn.*, **53**, 416 (2010)].
31. Loktionov E.Yu., Protasov Yu.Yu., Telekh V.D., Khaziev R.R. *Prib. Tekh. Eksp.*, (1), 53 (2013) [*Instrum. Experim. Techn.*, **56**, 46 (2013)].
32. Loktionov E.Yu., Ovchinnikov A.V., Protasov Yu.Yu., Sitnikov D.S. *Prib. Tekh. Eksp.*, (4), 140 (2010) [*Instrum. Experim. Techn.*, **53**, 596 (2010)].
33. Loktionov E.Yu., Ovchinnikov A.V., Protasov Yu.Yu., Sitnikov D.S. *Teplofiz. Vys. Temp.*, **49**, 415 (2011) [*High Temperature*, **49**, 404 (2011)].
34. Boulmer-Leborgne C., Benzerga R., Perrière J., in *Laser-Surface Interactions for New Materials Production* (Berlin–Heidelberg: Springer-Verlag, 2010).
35. Kasperczuk A., Pisarczyk T. *Opt. Appl.*, **31**, 571 (2001).
36. Zaidel' A.N., Ostrovskaya G.V. *Lazernye metody issledovaniya plazmy* (Laser Methods of Plasma Investigation) (Leningrad: Nauka, 1977).
37. Kolesnikov V.N. *Entsiklopediya nizkotemperaturnoi plazmy* (Encyclopedia of Low Temperature Plasma) Ed. by V.E. Fortov (Moscow: Yanus-K, 2006) p. 652.
38. Zel'dovichYa.B., Raizer Yu.P. *Physics of Shock Waves and High-Temperature Hydrodynamic Phenomena* (New York: Acad. Press, 1966, 1967; Moscow: Nauka, 1966) Vols 1 and 2.
39. Amoruso S., Wang X., Altucci C., de Lisio C., Armenante M., Bruzzese R., Spinelli N., Velotta R. *Appl. Surf. Sci.*, **186**, 358 (2002).
40. Hosoya N., Kajiwara I., Hosokawa T. *J. Sound and Vibration*, **331**, 1355 (2012).
41. Andreev S., Firsov K., Kazantsev S., Kononov I., Samokhin A. *Laser Phys.*, **17**, 834 (2007).
42. Borisenok V.A., Simakov V.G., Kuropatkin V.G., Bragunets V.A., Volgin V.A., Romaev V.N., Tukmakov V.V., Kruchinin V.A., Lebedeva A.A., Goncharova D.R., Zhernokletov M.V. *Prib. Tekh. Eksp.*, (4), 113 (2008).
43. Ionin A.A., Kudryashov S.I., Makarov S.V., Seleznev L.V., Sinitsyn D.V. *AIP Conf. Proc.*, **1464**, 138 (2012).
44. Pakhomov A.V., Gregory D.A., Thompson M.S. *AIAA J.*, **40**, 947 (2002).
45. Phipps C., Luke J., Funk D., Moore D., Glownia J., Lippert T. *Appl. Surf. Sci.*, **252**, 4838 (2006).
46. Loktionov E.Yu., Protasov Yu.S., Protasov Yu.Yu. *Usp. Prikl. Fiz.*, **1**, 439 (2013).
47. Grishin S.D., Leskov L.V. *Elektricheskie raketnye dvigateli kosmicheskikh apparatov* (Electric Rocket Engines of Space Vehicles) (Moscow: Mashinostroenie, 1989).
48. Le Harzic R., Breitling D., Weikert M., Sommer S., Föhl C., Dausinger F., Valette S., Donnet C., Audouard E. *Appl. Phys. A*, **80**, 1589 (2005).
49. Spiro A., Lowe M., Pasmanik G. *Appl. Phys. A: Mater. Sci. Proc.*, **107**, 801 (2012).
50. Cheng J., Perrie W., Sharp M., Edwardson S., Semaltianos N., Dearden G., Watkins K. *Appl. Phys. A: Mater. Sci. Proc.*, **95**, 739 (2009).
51. Torrisi L., Giuffrida L., Rosinski M., Schallhorn C. *Nucl. Instr. Meth. Phys. Res. B,* **268**, 2808 (2010).
52. Loktionov E.Yu., Ovchinnikov A.V., Protasov Yu.Yu., Sitnikov D.S. *Teplofiz. Vys. Temp.*, **48**, 766 (2010) [*High Temperature*, **48**, 729 (2010)].
53. Ancona A., Nodop D., Limpert J., Nolte S., Tünnermann A. *Appl. Phys. A: Mater. Sci. Proc.*, **94**, 19 (2009).
54. Pakhomov A.V., Roybal A.J., Duran M. *Appl. Spectrosc.*, **53**, 979 (1999).
55. Ye M., Grigoropoulos C.P. *Proc. SPIE Int. Soc. Opt. Eng.*, **4276**, 90 (2001).

56. *CRC Handbook of Chemistry and Physics.* Ed. by D.R.Lide (Boca Raton: Taylor and Francis, 2010).
57. D'Alessio L., Galasso A., Santagata A., Teghil R., Villani A.R., Villani P., Zaccagnino M. *Appl. Surf. Sci.*, **208–209**, 113 (2003).
58. Oh B., Kim D., Kim J., Lee J.-H. *J. Phys.: Conf. Ser.*, **59**, 567 (2007).
59. Stavropoulos P., Efthymiou K., Chryssolouris G. *Procedia CIRP*, **3**, 471 (2012).
60. Donnelly T., Lunney J., Amoruso S., Bruzzese R., Wang X., Ni X. *Appl. Phys. A: Mater. Sci. Proc.*, **100**, 569 (2010).
61. Ali D., Butt M.Z., Khaleeq-ur-Rahman M. *Appl. Surf. Sci.*, **257**, 2854 (2011).
62. Konomi I., Motohiro T., Asaoka T. *J. Appl. Phys.*, **106**, 013107 (2009).
63. Lin J. *Ph.D. Thesis* (Huntsville, Univesity of Alabama in Hunstsville, 2004).
64. Niemz M.H., in *Laser-Tissue Interactions* (Berlin–Heidelberg: Springer, 2007) p. 45.
65. Jang D.G., Kim M.S., Nam I.H., Uhm H.S., Suk H. *Appl. Phys. Lett.*, **99**, 141502 (2011).
66. Hermann J., Vivien C., Carricato A.P., Boulmer-Leborgne C. *Appl. Surf. Sci.*, **127–129**, 645 (1998).
67. Harilal S.S., Sizyuk T., Sizyuk V., Hassanein A. *Appl. Phys. Lett.*, **96**, 111503 (2010).
68. Uryupina D.S., Ivanov K.A., Brantov A.V., Savel'ev A.B., Bychenkov V.Y., Povarnitsyn M.E., Volkov R.V., Tikhonchuk V.T. *Phys. Plasmas*, **19**, 013104 (2012).
69. Hermann J., Boulmer-Leborgne C., Hong D. *J. Appl. Phys.*, **83**, 691 (1998).
70. Zhou Y., Gao Y., Wu B. *ASME Conf. Proc.*, **2010**, 203 (2010).
71. Haofeng H. et al. *J. Phys. D: Appl. Phys.*, **44**, 135202 (2011).
72. Fratanduono D.E., Boehly T.R., Celliers P.M., Barrios M.A., Eggert J.H., Smith R.F., Hicks D.G., Collins G.W., Meyerhofer D.D. *J. Appl. Phys.*, **110**, 073110 (2011).
73. Yang Y.-N., Yang B., Zhu J.-R., Shen Z.-H., Lu J., Ni X.-W. *Chinese Phys. B*, **17**, 1318 (2008).
74. Zheng Z.-y., Zhang Y., Zhao C.-c., Hao H.-y., Lu X., Li Y.-t., Zhang J. *Optoelectron. Lett.*, **3**, 394 (2007).
75. Wu B., Shin Y.C. *J. Appl. Phys.*, **101**, 103514 (2007).
76. Loktionov E.Yu., Ovchinnikov A.V., Protasov Yu.Yu., Sitnikov D.S. *Opt. Spektrosk*., **112**, 685 (2012) [*Opt. Spectrosc*., **112**, 631 (2012)].
77. Loktionov E.Yu., Ovchinnikov A.V., Protasov Yu.Yu., Sitnikov D.S. *Pis'ma Zh. Tekh. Fiz.*, **36**, 8 (2010) [*Techn. Phys. Lett*., **36**, 588 (2010)].
78. Phipps C.R., Turner T.P., Harrison R.F., York G.W., Osborne W.Z., Anderson G.K., Corlis X.F., Haynes L.C., Steele H.S., Spicochi K.C., King T.R. *J. Appl. Phys.*, **64**, 1083 (1988).
79. Zhou Y., Wu B., Forsman A. *J. Appl. Phys.*, **108**, 093504 (2010).
80. Phipps C.R., Luke J.R., Funk D.J., Moore D.S., Glownia J., Lippert T. *Proc. SPIE Int. Soc. Opt. Eng.*, **5448**, 1201 (2004).
81. Montagne J.E., Sarnet T., Prat C., Inglesakis G., Autric M. *Appl. Surf. Sci.*, **69**, 108 (1993).
82. Rosen D.I., Hastings D.E., Weyl G.M. *J. Appl. Phys.*, **53**, 5882 (1982).
83. Holmes B.S., Maher W.E., Hall R.B. *J. Appl. Phys.*, **51**, 5699 (1980).